


 Cite this: *RSC Adv.*, 2024, **14**, 15994

# Control and surveillance of redox potential for $^{233}\text{Pa}$ dissolution in $2\text{LiF}-\text{BeF}_2$ molten salt

 Zhongqi Zhao,<sup>ab</sup> Junxia Geng,<sup>ab</sup> Zhiqiang Cheng,<sup>ab</sup> Wenxin Li,<sup>ab</sup> Qiang Dou,<sup>ab</sup> Lan Zhang<sup>ab</sup> and Qingnuan Li<sup>\*ab</sup>

$^{233}\text{Pa}$ , the precursor nuclide of  $^{233}\text{U}$  in the thorium–uranium conversion is prone to reductive deposition in  $2\text{LiF}-\text{BeF}_2$  (66 : 34 mol%, FLiBe) molten salt. We explored the adjustment and control of the redox potential of the FLiBe melt to avoid the  $^{233}\text{Pa}$  reduction deposition. The experimental data indicated that the deposited  $^{233}\text{Pa}$  can be completely dissolved and reentered into the molten salt with the addition of oxidant  $\text{NiF}_2$ , and the distribution and behaviour of uranium, thorium, neptunium, and most fission products did not have any significant change in the  $\text{NiF}_2$ -oxidised FLiBe molten salt, showing the feasibility of this manner to make  $^{233}\text{Pa}$  exist stably in the melt. The effects of  $\text{NiF}_2$ -addition on the behaviour of the fission products  $^{95}\text{Nb}$  and  $^{131}\text{I}$  in the FLiBe molten salt were also investigated. It was found that  $^{131}\text{I}$  could be used as a redox indicator to monitor the redox potential of the oxidation-enhanced FLiBe molten salt. All the information drawn from this study could provide significant support for the control and surveillance of the redox potential of the FLiBe molten salt in the upcoming thorium molten salt reactor (TMSR).

Received 20th March 2024

Accepted 15th April 2024

DOI: 10.1039/d4ra02114b

[rsc.li/rsc-advances](https://rsc.li/rsc-advances)

## 1 Introduction

The molten salt reactor (MSR), a liquid-fuelled Generation IV reactor,<sup>1</sup> has come to the forefront of the international nuclear community because of its intrinsic characteristics suitable for the thorium–uranium fuel cycle.<sup>2–6</sup> In a thorium molten salt reactor (TMSR),  $^{232}\text{Th}$  can be converted to the fissile nuclide  $^{233}\text{U}$  by absorbing one neutron followed by two consecutive  $\beta^-$  decays. As the key intermediate nuclide in the thorium–uranium conversion,  $^{233}\text{Pa}$  has a relatively long half-life of 27 days, leading to its large accumulation in the TMSR. The high accumulation of  $^{233}\text{Pa}$  in the reactor, together with its relatively high neutron capture cross section, would cause an undesirable influence on the neutron economy of the reactor and the breeding rate of  $^{233}\text{U}$ .<sup>7</sup> Accordingly, it is necessary to remove  $^{233}\text{Pa}$  on time from the TMSR and then return it to TMSR after its conversion to  $^{233}\text{U}$ .<sup>3,4,7</sup>

We found that most of the  $^{233}\text{Pa}$  was deposited in the FLiBe melt and that the  $^{233}\text{Pa}$  activity decreased by 1 to 2 orders of magnitude after Hastelloy specimen or metallic Li were introduced.<sup>8</sup> Because of the similarity in the chemical properties of Pa and the fission product Nb, the decrease in  $^{233}\text{Pa}$  activity could be explained by reduction deposition, as mentioned in

the studies on the behaviour of fission products in the molten salt reactor experiment (MSRE) reported by Oak Ridge National Laboratory (ORNL). The recovery technique of  $^{233}\text{Pa}$  recommended by ORNL was based on the reduction extraction process of its metallic state. The separation factors of Pa against Th and RE could reach as high as 1200.<sup>9</sup> These results indicate the reductive nature of Pa.

Once the deposition of  $^{233}\text{Pa}$  occurs in the primary circuit of TMSR, the on-line removal of  $^{233}\text{Pa}$  from the fuel salt will not be achieved. More seriously, the accumulation of the fissile nuclide  $^{233}\text{U}$  in the  $^{233}\text{Pa}$  sediment would possibly cause overheating induced by the fission of  $^{233}\text{U}$  under neutron irradiation.<sup>7,8,10</sup> To operate the TMSR efficiently and safely, it is necessary to understand the behaviour of  $^{233}\text{Pa}$  in the FLiBe molten salt to prevent  $^{233}\text{Pa}$  deposition. Unfortunately, no information on the behaviour of  $^{233}\text{Pa}$  related with TMSR has been reported in ORNL's work, because the fertile material  $^{232}\text{Th}$  was not added into fuel salt during the development of their MSRE.

This paper reports the behaviour of  $^{233}\text{Pa}$  produced by irradiating thorium fluorides with photon neutron and how to make the deposited  $^{233}\text{Pa}$  dissolve and exist stably in the FLiBe molten salt by adjusting the redox potential of the salt with the oxidant  $\text{NiF}_2$ . The distribution and behaviour of several actinides and the fission products were examined in the oxidation-enhanced FLiBe molten salt. To monitor the redox potential of the oxidation-enhanced FLiBe molten salt, a surveillance protocol based on iodine fission product as redox indicators is proposed.

<sup>a</sup>Shanghai Institute of Applied Physics, Chinese Academy of Sciences, Shanghai 201800, China

<sup>b</sup>Centre of Excellence TMSR Energy System, Chinese Academy of Sciences, Shanghai 201800, China

<sup>\*</sup>University of Chinese Academy of Sciences, Beijing 100049, China


## 2 Experimental

The materials, apparatus, and methods described in our previous work were employed after minor modifications.<sup>8</sup> Briefly, ThF<sub>4</sub> powder (>99.5%, China National Nuclear Corporation) was mixed with LiF (99.85%, Sinopharm Chemical Reagent Co., Ltd.) and melted at 600 °C, followed by purification with H<sub>2</sub>/HF for 6 h to remove the possible oxides from this ThF<sub>4</sub>-LiF (FLiTh, mass ratio of 80 : 20) mixture. The LiF-BeF<sub>2</sub> eutectic salt (molar ratio of 66 : 34) was prepared by a similar method. The oxide content of both salt mixtures was determined to be approximately 100 ppm.

The FLiTh and UF<sub>4</sub> powders were sealed separately in two PMMA boxes and then irradiated on the photon neutron source driven by a 15 MeV electron linear accelerator for about three days. After cooling for about 24 h, the well mixed FLiTh/UF<sub>4</sub> powder of about 0.2 g was weighed accurately and measured directly with a calibrated HPGe detector (GMX30P4-70, ORTEC) to obtain the original inventory of radionuclides in the irradiated sample. 25.5 g of LiF-BeF<sub>2</sub> eutectic salt, 2.5 g of irradiated FLiTh, and 2.0 g of irradiated UF<sub>4</sub> were well mixed in a nickel crucible and then heated in a furnace mounted in an argon atmosphere glove box. The molten salt was maintained at 650 °C for at least 24 h and was ready for subsequent experiments. To examine the distribution and behaviour of <sup>233</sup>Pa in the oxidation-enhanced molten salt, NiF<sub>2</sub> powder (99.95%, Sinopharm Chemical Reagent Co., Ltd.) was added to the molten salt. The amounts of NiF<sub>2</sub> used for all the four experiments involved in this study are listed in Table 1. After each addition of NiF<sub>2</sub>, the salt was allowed to react completely for 8 h before sampling. Sampling was performed using the 5 mm inner diameter quartz tubes at intervals of 8 to 12 h. After cooling and weighing, the samples were subjected to measure the  $\gamma$ -spectra with the calibrated HPGe detectors.

The counting time of the  $\gamma$ -spectrum measurements varied from 0.5 h to 12 h, depending on the activity of the nuclides of interest. The nuclear data used for the nuclide identification and the activity calculation were provided by ENDF/B VIII.0,<sup>11</sup> and are listed in Table 2. The uncertainties in the activities mainly include the statistical error in the  $\gamma$ -ray counts, a 6% error in the detector efficiency, and an approximately 8% error in the sample geometry. The typical uncertainty for <sup>233</sup>Pa was about 12%. All the activity data were decay corrected to the start time point of each experiment.

## 3 Results and discussion

The redox condition of molten salts can be described in a variety of ways. D. Olander has suggested that the redox condition of

Table 1 The amounts of NiF<sub>2</sub> added in each experiment

Experiment	Times of NiF <sub>2</sub> added	Mass of NiF <sub>2</sub> in each addition, mg
Run 21-3	2	34.0, 71.0
Run 21-4	2	25.0, 57.0
Run 22-2	7	6.6, 8.8, 11.1, 9.1, 8.2, 11.5, 6.2
Run 22-3	5	1.8, 3.0, 4.9, 7.4, 13.0

Table 2 Nuclear data of the nuclides involved in this work

Nuclide	Half-life	Energy, keV	Intensity, %	Energy, keV	Intensity, %
<sup>233</sup> Pa	27.0 d	311.9	38.50	300.1	6.63
<sup>235</sup> U	7.04 × 10 <sup>8</sup> a	185.7	57.20	143.8	10.96
<sup>237</sup> U	6.75 d	208.0	21.20	164.6	1.86
<sup>239</sup> Np	2.36 d	277.6	14.44	228.2	11.14
<sup>228</sup> Ac	6.15 h	911.2	26.20	969.0	15.90
<sup>234m</sup> Pa	1.16 min	1001.9	0.84	766.4	0.32
<sup>141</sup> Ce	32.5 d	145.4	48.20	—	—
<sup>143</sup> Ce	1.38 d	293.3	42.80	664.6	5.69
<sup>140</sup> Ba	12.8 d	537.3	24.39	162.7	6.22
<sup>95</sup> Nb	35.0 d	765.8	99.81	—	—
<sup>95</sup> Zr	64.0 d	756.7	54.38	724.2	44.27
<sup>99</sup> Mo	2.75 d	739.5	12.26	181.1	6.14
<sup>99m</sup> Tc	6.01 h	140.5	89.00	—	—
<sup>103</sup> Ru	39.2 d	497.1	91.00	610.3	5.76
<sup>132</sup> Te	3.20 d	228.2	88.00	49.7	14.96
<sup>132</sup> I	2.30 h	667.7	98.70	772.6	75.60
<sup>131</sup> I	8.03 d	364.5	81.50	284.3	6.12

molten fluoride salts should be defined quantitatively as the chemical potential of fluorine,<sup>12</sup> whereas it is common to express the redox condition in terms of redox potential. Redox potential is defined as the tendency of a chemical species to lose electrons and become oxidised (or gain electrons and become reduced), and it can be obtained directly from experimental measurements, or it can be calculated from the Nernst equation using the standard electrode potential and the activities of the oxidised and reduced species. This study does not include any electrochemical measurements, but only a simple estimation of the redox potential from reference data.

For the fuel salt containing UF<sub>4</sub>, where the U<sup>4+</sup>/U<sup>3+</sup> couple is dominant, the redox potential can be conveniently measured and controlled by the U<sup>4+</sup>/U<sup>3+</sup> mole ratio. According to ORNL reports, the electrode potentials of U<sup>4+</sup>/U<sup>3+</sup>, NbF<sub>5</sub>(g)/Nb, I(g)/I<sup>-</sup> and Ni<sup>2+</sup>/Ni are -1.106 V, -0.311 V, -0.051 V and 0.409 V (vs. HF(g)/H<sub>2</sub>, F<sup>-</sup> in FLiBe) at 650 °C, respectively.<sup>13</sup> Therefore, NiF<sub>2</sub> can be used as an oxidant, and the redox condition of the molten salt can also be roughly described by the amount of NiF<sub>2</sub> added.

### 3.1 Oxidative dissolution of <sup>233</sup>Pa

Two parallel experiments were carried out, in each of which NiF<sub>2</sub> was added to the molten salt twice, 34 mg and 71 mg in one experiment (run 21-3) and 25 mg and 57 mg in the other (run 21-4). Each experiment lasted for about 8 days, and the specific activities of some selected nuclides in the melt were determined. After correction for the decay of the radionuclides, the nuclide specific activities with the addition of NiF<sub>2</sub> from two experiments were obtained, and depicted in Fig. 1(a) and (b).

The specific activity of <sup>233</sup>Pa in the FLiBe melt decreased obviously when compared to the expected value based on the experimentally determined inventory. The large decrease in <sup>233</sup>Pa activity confirms the observation in our previous work.<sup>8</sup> Furthermore, the behaviour of the steep decrease in <sup>233</sup>Pa activity is similar to that of the typical noble fission product



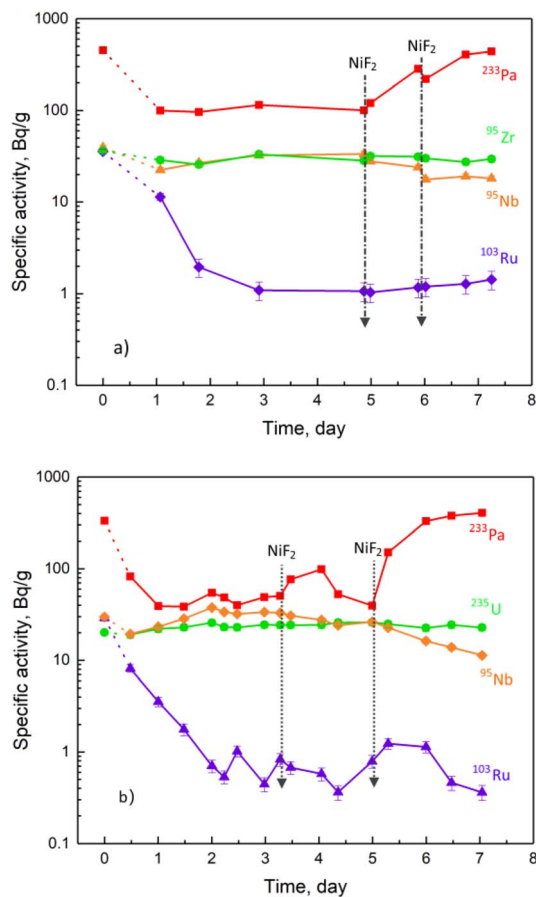
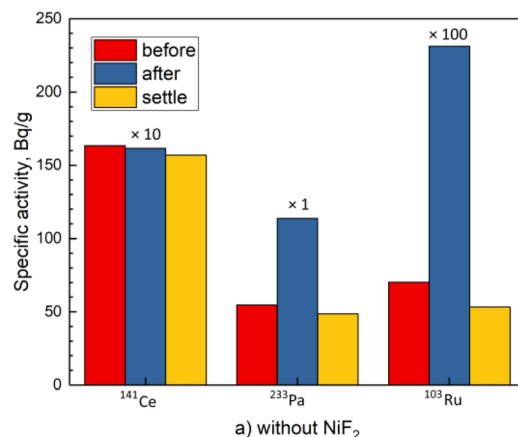
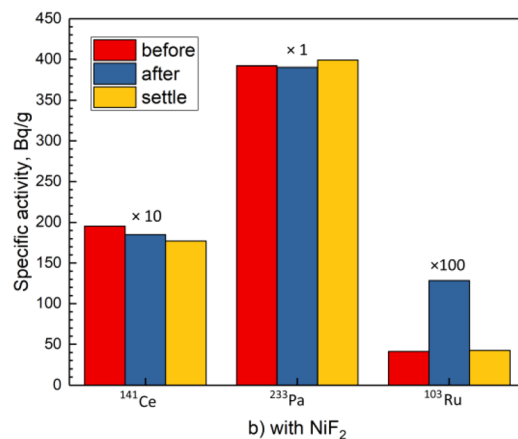


Fig. 1 Specific activities of selected nuclides in FLiBe molten salt. (a) Run 21-3, (b) run 21-4.



a) without  $\text{NiF}_2$

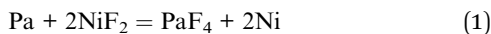


b) with  $\text{NiF}_2$

Fig. 2 Specific activities of  $^{233}\text{Pa}$ ,  $^{103}\text{Ru}$  and  $^{141}\text{Ce}$  in molten salt before and after stirring. (a) Without  $\text{NiF}_2$ ; (b) with  $\text{NiF}_2$ .

$^{103}\text{Ru}$ . The decrease in  $^{233}\text{Pa}$  activity should result from reduction followed by deposition in the form of metal granules, similar to the noble metal fission products.<sup>14</sup>

In addition, the increase in the redox potential resulting from the addition of  $\text{NiF}_2$  to the melt could be an approach to eliminating the reductive deposition of  $^{233}\text{Pa}$ . As seen also from Fig. 1, the specific activity of  $^{233}\text{Pa}$  increased significantly with the addition of the oxidant  $\text{NiF}_2$ . When sufficient  $\text{NiF}_2$  was added, the specific activity of  $^{233}\text{Pa}$  could match the value calculated from the inventory, exhibiting the ability of the oxidant  $\text{NiF}_2$  to oxidise the deposited Pa to a soluble compound, most likely,  $\text{PaF}_4$ .



To further demonstrate the deposition of  $^{233}\text{Pa}$  in the melt and its dissolution after the addition of  $\text{NiF}_2$ , the test molten salt containing  $^{233}\text{Pa}$  and the fission products was stirred thoroughly with a graphite rod and then allowed to settle for several hours. Three samples were taken from the molten salt at different moments, *i.e.*, before stirring, immediately after stirring, and 4 hours later after stirring, respectively. The same procedure was repeated for the other test molten salt, where  $\text{NiF}_2$  was added beforehand. The measurements of the specific

activity obtained from the experiments are shown in Fig. 2 for the nuclides  $^{141}\text{Ce}$ ,  $^{233}\text{Pa}$  and  $^{103}\text{Ru}$ .

As indicated in our previous work,<sup>8</sup> the deposited  $^{233}\text{Pa}$  and the noble metal fission products were distributed mainly in the bottom of the molten salt. When the molten salt was stirred thoroughly, the precipitates were dispersed throughout the entire melt in the form of small granules, resulting in an obvious increase in the activities of these nuclides. After settling for several hours, these small granules sink, and their activities in the melt decreased to the original level, as shown in Fig. 2(a) for  $^{233}\text{Pa}$  and  $^{103}\text{Ru}$ . In contrast, the specific activity of the salt-seeking fission product, represented by  $^{141}\text{Ce}$ , did not change no matter whether stirred or settled, due to its good solubility in the molten salt.

In the experiment where the oxidant  $\text{NiF}_2$  was added into the FLiBe molten salt beforehand, the pattern of  $^{103}\text{Ru}$ 's specific activities was the same as before, implying that  $^{103}\text{Ru}$  behaved as a typical noble metal fission product even in oxidation-enhanced melt. However, a significant variation in the specific activities of  $^{233}\text{Pa}$  occurred after the oxidant  $\text{NiF}_2$  was added. At this time,  $^{233}\text{Pa}$  behaved more like  $^{141}\text{Ce}$  rather than  $^{103}\text{Ru}$  and its specific activity remained unchanged no matter whether stirred or settled (Fig. 2(b)), implying a complete dissolution of



$^{233}\text{Pa}$  in the oxidation-enhanced melt resulting from the addition of  $\text{NiF}_2$ . It can be concluded that the increase in the redox potential of the FLiBe molten salt was able to eliminate the deposition of  $^{233}\text{Pa}$  or to promote the re-dissolution of the deposited  $^{233}\text{Pa}$ . Consequently, maintaining the redox potential at a suitably high level is essential to the oxidative dissolution of  $^{233}\text{Pa}$ .

### 3.2 Behaviour of actinides in the $\text{NiF}_2$ -oxidised FLiBe molten salt

ORNL has made great efforts to study the behaviour and distribution of radioactive nuclides in the MSRE<sup>14–17</sup> because of their importance to the performance and safety of the MSRE operation. As mentioned above, the redox potential of the FLiBe molten salt in the TMSR should be maintained at a higher level than that in the MSRE to eliminate the possible deposition of  $^{233}\text{Pa}$  in the TMSR. Therefore, it is necessary to clarify whether the distribution and behaviour of the actinides and fission products in the oxidation-enhanced FLiBe molten salt have any negative impact on the operation of the TMSR.

As shown in Fig. 1(b), the specific activity of the long-lived nuclide  $^{235}\text{U}$  remained constant after sufficient  $\text{NiF}_2$  was added, indicating an independent behaviour of uranium on the redox potential in the FLiBe molten salt. In another experiment (run 22-2), a total amount of 61.5 mg of  $\text{NiF}_2$  was added to molten salt, and the specific activities of four actinides,  $^{237}\text{U}$ ,  $^{239}\text{Np}$ ,  $^{234\text{m}}\text{Pa}$  and  $^{228}\text{Ac}$ , are shown in Fig. 3.  $^{237}\text{U}$  is the product of the  $^{238}\text{U}$  ( $n, 2n$ ) reaction,  $^{239}\text{Np}$  is the decay daughter of  $^{239}\text{U}$  produced by the  $^{238}\text{U}$  ( $n, \gamma$ ) reaction,  $^{234\text{m}}\text{Pa}$  is the daughter of  $^{234}\text{Th}$  produced by the  $\alpha$ -decay of  $^{238}\text{U}$ , and  $^{228}\text{Ac}$  is the daughter of  $^{228}\text{Ra}$  produced by the  $\alpha$ -decay of  $^{232}\text{Th}$ . When the oxidant  $\text{NiF}_2$  was gradually added to the molten salt, their specific activities remained constant, indicating the stable existence of their precursors, *i.e.*, U, Np, and Th, in the melt, which were not affected by the addition of  $\text{NiF}_2$ . Therefore, the increase in redox potential would not cause an undesirable change in the distribution and behaviour of these actinides in the FLiBe molten salt.

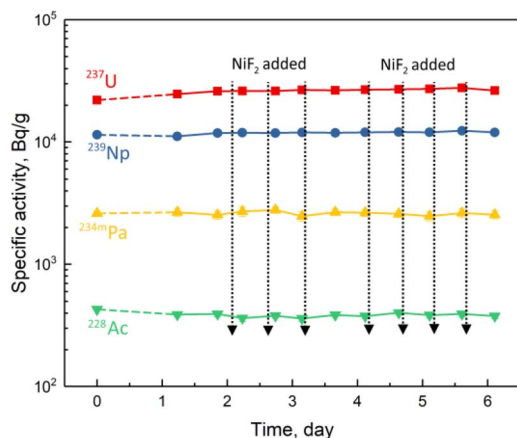


Fig. 3 Specific activities of the actinides in FLiBe molten salt with the addition of  $\text{NiF}_2$ .

### 3.3 Behaviour of fission products in the $\text{NiF}_2$ -oxidised FLiBe molten salt

According to the behaviour in the FLiBe molten salt of MSRE, ORNL classified the fission products into three categories, *i.e.*, the gas fission products, the salt-seeking fission products, and the noble metal fission products.<sup>14–17</sup> Among them, the salt-seeking fission products could dissolve well in the FLiBe molten salt and remain stable. In the experiment mentioned above, the specific activities of the typical salt-seeking fission products,  $^{95}\text{Zr}$ ,  $^{141}\text{Ce}$ ,  $^{143}\text{Ce}$  and  $^{140}\text{Ba}$ , were determined and shown in Fig. 4. No significant variation in their specific activities was observed, indicating the stable presence of these salt-seeking fission products in the  $\text{NiF}_2$ -oxidised FLiBe melt.

Compared to the salt-seeking fission products, the variation of the specific activities of the noble metal fission products, such as  $^{99\text{m}}\text{Tc}$ ,  $^{99}\text{Mo}$ ,  $^{103}\text{Ru}$  and  $^{132}\text{Te}$ , showed a quite different pattern. As shown in Fig. 5, their specific activities decreased rapidly by more than one order of magnitude before the addition of  $\text{NiF}_2$ , which is very similar to that of  $^{233}\text{Pa}$  shown in Fig. 1. On the other hand, the variation in specific activity

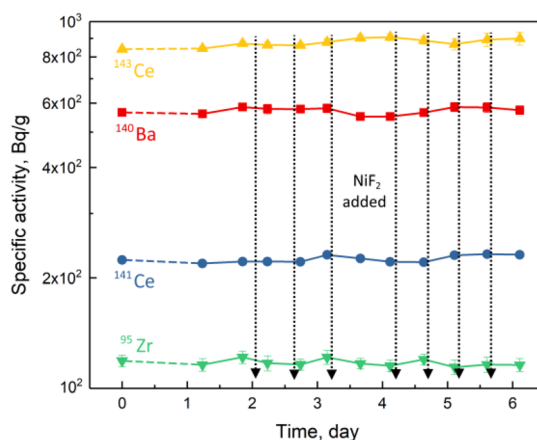


Fig. 4 Specific activities for the salt-seeking fission products in FLiBe molten salt with the addition of  $\text{NiF}_2$ .

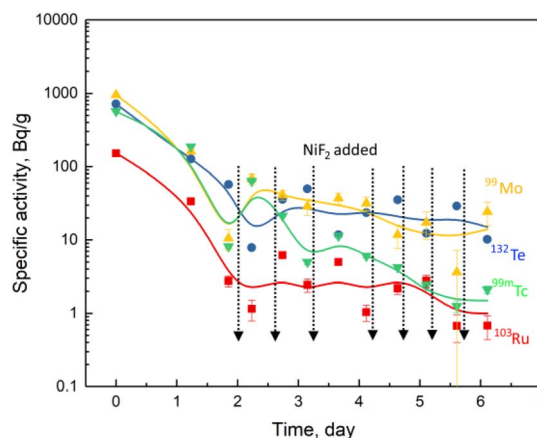


Fig. 5 Specific activities for the noble metal fission products in FLiBe molten salt with the addition of  $\text{NiF}_2$ .





during the over period of  $\text{NiF}_2$  addition was different from  $^{233}\text{Pa}$ . No increase in the specific activity of the noble metal fission products was found with the continuous addition of  $\text{NiF}_2$ . As a result, their specific activities were found to be widely scattered and fluctuated at a low activity level due to the large statistical errors of the  $\gamma$ -counts. The different effects of the specific activities on  $\text{NiF}_2$  addition between the  $^{233}\text{Pa}$  and the noble metal fission products implicates that the latter were more difficult to oxidise by  $\text{NiF}_2$  and redissolved in the melt. Thus, the behaviour and distribution of noble metal fission products in the  $\text{NiF}_2$ -oxidised FLiBe molten salt were not significantly different from those observed by ORNL in the MSRE.<sup>14,16</sup> After sufficient  $\text{NiF}_2$  was added, the noble metal fission products remained in the form of sediment, while  $^{233}\text{Pa}$  was already oxidised and dissolved in the molten salt.

### 3.4 Control and monitoring of the redox potential in $\text{NiF}_2$ -oxidised FLiBe molten salt

As mentioned above, the deposition of  $^{233}\text{Pa}$  in the FLiBe melt could be eliminated by increasing the redox potential of the melt, and the increase in redox potential did not essentially change the behaviour and distribution of U, Np, Th, and most fission products. It is therefore not only necessary but also feasible to increase the redox potential of the FLiBe melt. Thus, the issues are how to control the desired range of the redox potential and how to monitor the redox potential in the FLiBe melt of TMSR.

Electrochemical measurements of redox potential are time consuming, and the optical spectroscopy techniques for determining the  $\text{U}^{4+}/\text{U}^{3+}$  mole ratio may be limited due to the corrosive nature of fluoride salts.<sup>18</sup> A strategy worth exploring is to use the behaviour of specific fission products to detect or assess the redox potential of the molten salt, *i.e.*, to use the fission products as redox indicators.

**3.4.1  $^{95}\text{Nb}$  used as a redox indicator in  $\text{NiF}_2$ -oxidised FLiBe molten salt.**  $^{95}\text{Nb}$  is a high-yield daughter of the fission product  $^{95}\text{Zr}$  and has a unique characteristic in its chemical behaviour. As reported in the ORNL reports,<sup>14–17</sup> when the MSRE was operated with  $^{235,238}\text{UF}_4$  fuel,  $^{95}\text{Nb}$  behaved as a typical noble metal fission product and deposited, as NbC form, on the reactor's graphite moderator, with no activity detected in the FLiBe melt. However, when the MSRE was operated with  $^{233}\text{UF}_4$  fuel,  $^{95}\text{Nb}$  was observed in the fuel salt. At the same time, the corrosion of the structural materials of the reactor was exacerbated, implying an increase in the redox potential of the melt. To inhibit the corrosion induced by oxidation, metallic beryllium was frequently added to the MSRE to reduce the redox potential of the melt. The results of the *in situ* measurement showed that the activity of  $^{95}\text{Nb}$  in the molten salt decreased with decreasing redox potential. Thus, the dependence of the  $^{95}\text{Nb}$  activity in the FLiBe molten salt on the redox potential of the melt suggests that the fission product  $^{95}\text{Nb}$  could be used as an radiochemical indicator of the redox potential in the MSRE.<sup>14–17,19</sup>

As recommended by ORNL, appropriate values of the  $\text{U}^{4+}/\text{U}^{3+}$  mole ratio were set in the range of 10–100 to prevent the

formation of uranium carbide and to mitigate the corrosion of the structural materials of the MSRE.<sup>15</sup> However, in the present work it was shown that the redox potential of the melt had to be adjusted to a higher level to avoid the deposition of  $^{233}\text{Pa}$ . In such a situation, the question is whether  $^{95}\text{Nb}$  could still be used as a redox indicator in the  $\text{NiF}_2$ -oxidised FLiBe molten salt.

A positive conclusion would be drawn from the experimental results shown in Fig. 1. Contrary to the increase of the  $^{233}\text{Pa}$  activity in the molten salt, the  $^{95}\text{Nb}$  activity decreased with the addition of the oxidant  $\text{NiF}_2$ . The addition of 105 mg  $\text{NiF}_2$  increased the activity of  $^{233}\text{Pa}$  by a factor of 5, while the activity of  $^{95}\text{Nb}$  decreased by about 50%. The decrease in  $^{95}\text{Nb}$  activity may be attributed to the oxidation of dissolved  $\text{NbF}_4$  to volatile  $\text{NbF}_5$  by the addition of  $\text{NiF}_2$ , followed by the evaporation of  $\text{NbF}_5$  at high temperature.<sup>20</sup> ORNL calculations indicated that Nb could be oxidised and volatilised from the molten salt at a redox potential corresponding to a  $\text{U}^{4+}/\text{U}^{3+}$  mole ratio greater than  $10^4$ .<sup>13</sup> Therefore, if the activity of  $^{95}\text{Nb}$  in the molten salt decreases while  $^{95}\text{Nb}$  can be detected in the gas phase, it suggests that the molten salt is under oxidising condition. In other words,  $^{95}\text{Nb}$  could still be able to be used as a redox indicator in oxidation-enhanced FLiBe melt. However, its low sensitivity to the redox potential of the melt might more or less limit its practical application compared to iodine fission products as seen below.

**3.4.2  $^{131}\text{I}$  used as a redox indicator in  $\text{NiF}_2$ -oxidised FLiBe molten salt.** Iodine isotopes are high-yield fission products with a wide range of mass numbers, and their decay characteristics are well suited to analysis by  $\gamma$ -ray spectroscopy. In addition, the iodine element has multiple chemical valences ranging from  $-1$  to  $+7$ , implying a strong dependence of its behaviour on the redox potential of the molten salt.

The behaviour of iodine fission products and their correlation with the redox potential in the FLiBe molten salt have been studied in our previous work.<sup>21,22</sup> The investigations showed that as the redox potential of the molten salt increases, the iodine is oxidised into the iodine molecule  $\text{I}_2$  and released from the salt, leading to a decrease in the iodine activity remaining in the melt. In the present work, two parallel experiments were carried out, where the specific activities of  $^{131}\text{I}$  and  $^{233}\text{Pa}$  in the FLiBe and their correlation with the redox potential were examined simultaneously (Fig. 6). Similar to Fig. 1, the specific activity of  $^{233}\text{Pa}$  increased to the inventory value with the addition of  $\text{NiF}_2$  due to its oxidative dissolution in the molten salt. In contrast, the specific activity of  $^{131}\text{I}$  decreased continuously with the addition of  $\text{NiF}_2$  due to its oxidation and subsequent volatilisation. It should be noted that when  $^{233}\text{Pa}$  was completely dissolved and returned to the salt, almost no  $^{131}\text{I}$  was present in the molten salt any longer. Furthermore, the variation in the specific activities of  $^{131}\text{I}$  was much larger than that of  $^{95}\text{Nb}$  when  $\text{NiF}_2$  was added, suggesting that the sensitivity of  $^{131}\text{I}$ , as a redox indicator, was better than that of  $^{95}\text{Nb}$ . Consequently,  $^{131}\text{I}$  could be used as an indicator to monitor the deposition of  $^{233}\text{Pa}$  in the FLiBe melt.

The chemical principle that allows the fission product iodine to be used as a redox indicator is based on its volatility caused by oxidation. ORNL evaluated the correlation between the redox



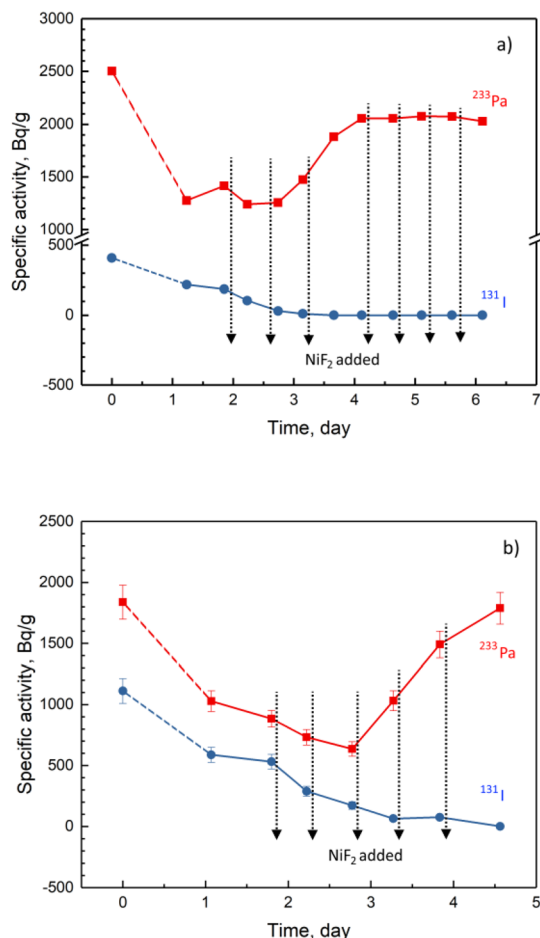


Fig. 6 Specific activities of  $^{131}\text{I}$  and  $^{233}\text{Pa}$  in FLiBe molten salt with the addition of  $\text{NiF}_2$ . The amount of  $\text{NiF}_2$  in each addition: (a) run 22-2; (b) run 22-3.

potential of the FLiBe melt and the oxidation of iodine and indicated that when massive  $\text{I}^-$  ions were oxidised and volatilised, the redox potential of the melt corresponded to a  $\text{U}^{4+}/\text{U}^{3+}$  mole ratio of  $10^8$ ,<sup>13</sup> even higher than the  $10^4$  mentioned above for  $^{95}\text{Nb}$ . Although large differences exist for the  $\text{U}^{4+}/\text{U}^{3+}$  mole ratios estimated from different indicators of iodine and niobium, it can be inferred that the  $\text{U}^{4+}/\text{U}^{3+}$  mole ratio in the FLiBe melt should be controlled to be in the range of  $10^4$  to  $10^8$ , significantly higher than the  $\text{U}^{4+}/\text{U}^{3+}$  mole ratio of 10 to  $10^2$  proposed by ORNL for their MSRE. To monitor the redox potential of the melt, the electrochemical method or the spectral method might suffer from the difficulty related to the huge difference in the concentration between  $\text{U}^{4+}/\text{U}^{3+}$ .<sup>18</sup> Consequently, it would be preferable to use fission product  $^{131}\text{I}$  as a redox indicator to adjust and monitor the redox potential of the FLiBe melt for  $^{233}\text{Pa}$  dissolution.

As indicated above, increasing redox potential of the FLiBe melt may not change the behaviour of Th, U, Np, and most of the fission products present in TMSR, but some of the possible influences on the operation of TMSR should be further evaluated.  $^{135}\text{Xe}$ , the most important neutron poison, is the daughter of  $^{135}\text{I}$ . The ORNL report indicated that the residual  $^{135}\text{Xe}$  in the

reactor was strongly dependent on the removal rate of  $^{135}\text{I}$  from the molten salt, *i.e.*, the more iodine was removed, the less  $^{135}\text{Xe}$  remained in the molten salt.<sup>14,15,23</sup> Thus, increasing the redox potential of the FLiBe melt would remarkably raise the neutron economy of the reactor.

On the other hand, however, the escape of iodine fission products caused by the higher oxidation potential would also lead to the loss of some of the delayed neutron precursors of the iodine isotopes, such as  $^{137-140}\text{I}$  with very short half-lives, which will bring about a kind of issues in the control of reactor to some extent. In addition, the increase in the redox potential of the melt might exacerbate the corrosion of the Hastelloy structural materials of the reactor. Therefore, it is necessary to further investigate and evaluate the influence of increasing the redox potential of the FLiBe molten salt on the efficiency and safety of TMSR operation.

## 4 Conclusions

To eliminate the reductive deposition of the key nuclide  $^{233}\text{Pa}$  in the thorium–uranium conversion, a method of increasing the redox potential of the FLiBe molten salt was proposed for the first time. The experimental results obtained from these studies again showed a great deposition of  $^{233}\text{Pa}$  in the FLiBe molten salt, and the addition of  $\text{NiF}_2$  could promote the complete dissolution of the deposited  $^{233}\text{Pa}$ . No adverse changes in the distribution and behaviour of Th, U, Np, and most of the fission products were found in the  $\text{NiF}_2$ -oxidised FLiBe molten salt. In the  $\text{NiF}_2$ -oxidised FLiBe molten salt, the fission products  $^{95}\text{Nb}$  and  $^{131}\text{I}$ , especially the latter, could be used as suitable redox indicators. The results obtained from these studies would have significant reference value for the development and operation of TMSR. However further studies are required using the actual fuel salt from the upcoming TMSR.

## Conflicts of interest

There are no conflicts to declare.

## Acknowledgements

The authors would like to express their sincere thanks to the Free Electron Group for their encouragement and help. This work was supported by the “Strategic Priority Research Program” (XDA02030000), “Frontier Science Key Program” (QZYDYSSW-JSC016), “the Young Potential Program of Shanghai Institute of Applied Physics, Chinese Academy of Sciences” (E0552901), “National Natural Science Foundation of China” (No. 12175303 and U2267226) and “Xinjiang Uygur Autonomous Region Key R&D Task Special Project” (2022B01039).

## Notes and references

- 1 U.S. Department of Energy, *Phil. Rev.*, 2002, **66**, 239–241.
- 2 L. Mathieu, D. Heuer, R. Brissot, C. Garzenne, C. Le Brun, D. Lecarpentier, E. Liatard, J. M. Loiseaux, O. Méplan,



- E. Merle-Lucotte, A. Nuttin, E. Walle and J. Wilson, *Prog. Nucl. Energy*, 2006, **48**, 664–679.
- 3 R. C. Robertson, *MSRE Design & Operations Report Part 1 Description of Reactor Design*, ORNL-TM-728, 1965.
- 4 R. C. Robertson, *Conceptual Design Study of a Single-Fluid Molten-Salt Breeder Reactor*, ORNL-4541, 1971.
- 5 *Advanced Reactor Concepts, Technical Review Panel Report: Evaluation and Identification of Future R&D on Eight Advanced Reactor Concepts, Conducted April–September 2012*, United States, 2012.
- 6 Department for Business Innovation & Skills, *Nuclear Industrial Strategy*, <https://www.gov.uk/government/collections/nuclear-industrial-strategy>.
- 7 W. Li and Q. Li, *J. Nucl. Radiochem.*, 2016, **38**, 327–336.
- 8 Z. Zhao, J. Hu, Z. Cheng, J. Geng, W. Li, Q. Dou, J. Chen, Q. Li and X. Cai, *RSC Adv.*, 2021, **11**, 7436–7441.
- 9 L. M. Ferris, J. C. Mailen, J. J. Lawrence, F. J. Smith and E. D. Nogueira, *J. Inorg. Nucl. Chem.*, 1970, **32**, 2019–2035.
- 10 A. M. Weinberg, *The First Nuclear Era: The Life and Times of a Technological Fixer*, American Institute of Physics, New York, NY, United States, 1994.
- 11 M. B. Chadwick, D. A. Brown, R. Capote, *et al.*, *Nucl. Data Sheets*, 2018, **148**, 1–142.
- 12 D. Olander, *J. Nucl. Mater.*, 2002, **300**, 270–272.
- 13 C. F. Baes Jr, *Nucl. Metall.*, 1969, **15**, 617–644.
- 14 E. L. Compere, S. S. Kirslis, E. G. Bohlmann, F. F. Blankenship and W. R. Grimes, *Fission Product Behavior in the Molten Salt Reactor Experiment*, ORNL-4865, 1975.
- 15 R. E. Thoma, *Chemical Aspects of MSRE Operations*, ORNL-4658, 1971.
- 16 R. J. Kedl, *Migration of a Class of Fission Products (Noble Metals) in the Molten-Salt Reactor Experiment*, ORNL-TM-3884, 1972.
- 17 W. R. Grimes, *Nucl. Appl. Technol.*, 1970, **8**, 137–155.
- 18 J. Zhang, C. W. Forsberg, M. F. Simpson, S. Guo, S. T. Lam, R. O. Scarlat, F. Carotti, K. J. Chan, P. M. Singh, W. Doniger, K. Sridharan and J. R. Keiser, *Corros. Sci.*, 2018, **144**, 44–53.
- 19 Z. Cheng, Z. Zhao, J. Geng, W. Li, Q. Dou and Q. Li, *J. Nucl. Mater.*, 2022, **566**, 153807.
- 20 J. H. Junkins, R. L. Farrar Jr, E. J. Barber and H. A. Bernhardt, *J. Am. Chem. Soc.*, 1952, **74**, 3464–3466.
- 21 J. Geng, Z. Zhao, Z. Cheng, W. Li, Q. Dou, H. Fu, J. Hu, X. Cai, J. Chen and Q. Li, *RSC Adv.*, 2021, **11**, 22611–22617.
- 22 J. Geng, Z. Zhao, Z. Cheng, W. Li, Q. Dou and Q. Li, *Inorg. Chem.*, 2022, **61**, 7406–7413.
- 23 M. W. Rosenthal, P. N. Haubenreich and R. B. Briggs, *Development Status of Molten-Salt Breeder Reactors*, ORNL-4812, 1972.

